(Received 20 August 2025, Accepted 3 December 2025, Scheduled 18 December 2025)

Inertial Forces from Relativistic and Thermal Effects of Electromagnetic Frequency Sweeps

Roberto B. B. Ovando*

Independent Researcher

ABSTRACT: We investigate the thermal and relativistic effects produced when an electrically conductive object is moving in tandem with a source of a variable electromagnetic field. First, we derive an energy-frequency relation to quantify the temperature rise induced by such a field. This relation is then combined with the Lorentz-Fitzgerald contraction and time dilation from special relativity to identify a force, F_c, required to reconcile energy conservation between stationary and moving observers. We further relate F_c to the relativistic energy of a moving mass, extending the analysis to objects without electrical conductivity. This connection leads to the prediction of an inertial force F_{cf} generated by the frequency sweep of an electromagnetic wave (whether caused by relative motion or by internal modulation) that interacts with mass regardless of its electrical properties.

1. INTRODUCTION

The study of relative motion between electrically charged bodies and sources of electromagnetic fields underpins many fundamental principles in both low and high energy physics [1]. The electrodynamics of moving bodies has been addressed through classical Galilean transformations as well as Minkowski spacetime formulations [2]. Pre-relativistic investigations predicted that charged bodies contract along the axis of motion [3]. Notably, Heaviside examined the electromagnetic effects of a moving charge under the assumption of an invariable surface charge distribution [3], while Searle [4] demonstrated that a charged sphere in motion contracts in the direction of travel, producing a field distribution similar to that of a charged ellipsoid.

Le Bellac and Levy Leblond [5] developed a Galilean-invariant formulation of electromagnetism by identifying two distinct non-relativistic limits for the electric and magnetic fields. Building on this framework, De Montigny and Rousseaux [6] applied a Riemann-Lorenz formulation to reinforce these results in the context of low energy phenomena and the electrodynamics of bodies moving at low velocities. Relativistic effects in electromagnetism have also been examined in [7], demonstrating that the magnetic component of the Lorentz force emerges directly from the application of Lorentz contraction in the analysis of electrical currents. More recently, studies in time-varying media [8] have shown that, for any stationary observer, an accelerated electromagnetic wave exhibits relativistic effects with respect to laboratory time.

This study examines how a stationary observer measures the heat generated in an electrically conductive object moving in tandem with a source of a variable electromagnetic field. The analysis incorporates the Lorentz-Fitzgerald contraction and time dilation to ensure that energy conservation is maintained between the thermal measurements of stationary and moving observers. The principal contribution of this work is the identification of a new inertial force, F_{cf}, that arises from frequency sweeps in electromagnetic fields. This force represents a relativistic coupling between field energy and inertia, emerging as a direct consequence of Lorentz-Fitzgerald contraction, time dilation, and the requirement of energy conservation. F_{cf} acts on matter regardless of electrical conductivity providing a potential mechanism for non-contact particle manipulation and frequency driven propulsion systems.

2. ENERGY-FREQUENCY CHARACTERIZATION OF JOULE HEATING FROM VARIABLE ELECTROMAGNETIC FIELDS

Joule power losses arise from the conduction of electric current through electrically conductive materials. These losses generate heat, raising the temperature of the conductor, which is subsequently transferred to surrounding media via conduction, convection, and radiation mechanisms [9].

The Joule power loss per unit surface area $\bar{P}$ (W/m^2) produced by induced electric currents in an electrically conductive object is given by

$$\bar{P} = \int_0^y \rho \cdot J_z^2 dy \tag{1}$$

where ρ is the electrical resistivity of the material (Ωm), and J_z is the current density (A/m^2) along the z direction (see Fig. 1).

For a sinusoidal source of variable electromagnetic field, the distribution of current density J_z is

$$J_z = J_o e^{-y/\alpha_{sk}} \cos\left(2\pi f t - y/\alpha_{sk}\right) \tag{2}$$

* Corresponding author: Roberto Bernardo Benedicto Ovando (ovandor@ieee.org).

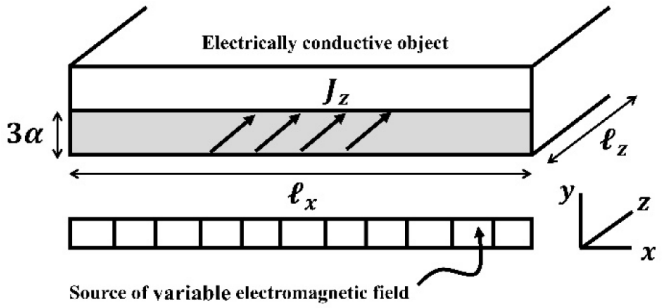

FIGURE 1. Cross-sectional area occupied by the current density J_z.

where J_o is the peak current density (A/m^2) [10], f the frequency of the source of variable electromagnetic field (Hz), t is time (s), and α_{sk} the skin depth of penetration (m) defined as

$$\alpha_{sk} = \sqrt{\frac{\rho}{\pi \mu f}} \tag{3}$$

with μ denoting the magnetic permeability (H/m).

Substituting Eq. (2) with Eq. (1) yields

$$\bar{P}(y) = \frac{\rho J_o^2 \alpha_{sk}}{4}\left(1 - e^{-2y/\alpha_{sk}}\right) \tag{4}$$

From Eq. (4), it is evident that most of the induced power loss is confined within approximately three skin depths (Fig. 2) [10]. Beyond this depth, the exponential attenuation of the electromagnetic field significantly reduces the current density and, consequently, the generated heat [10].

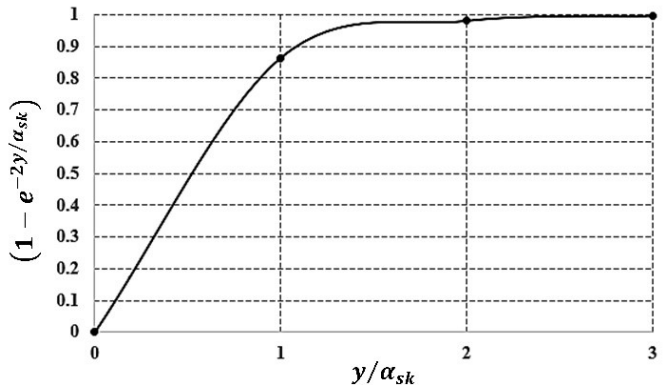

FIGURE 2. Induced power loss distributes within approximately three skin depths.

Thus, extending the integral to ∞ gives an accurate estimate of the total Joule power loss per unit surface area:

$$\bar{P} = \int_0^{\infty} \rho \cdot J_z^2 dy = \frac{\rho J_o^2 \alpha_{sk}}{4} \tag{5}$$

For practical applications, it is convenient to express the results in terms of the total electric current $I(t)$ flowing through a surface of width l_x:

$$I(t) = l_x \int_0^{\infty} J_z dy \tag{6}$$

Solving the integral using Eq. (2) gives

$$I(t) = \frac{l_x J_o \alpha_{sk}}{\sqrt{2}} \cos\left(2\pi f t - \frac{\pi}{4}\right) \tag{7}$$

The RMS (Root Mean Square) current follows as

$$I_{rms} = \sqrt{\frac{1}{T}\int_0^T I^2(t)\, dt} = \frac{l_x J_o \alpha_{sk}}{2} \tag{8}$$

where T is the period of the signal.

Equation (8) leads to

$$J_o = \frac{2 I_{rms}}{\alpha_{sk} l_x} \tag{9}$$

Substituting Eq. (9) into Eq. (5) and multiplying by the total external surface area $l_x \cdot l_z$, the total Joule power loss becomes

$$P_{loss} = R(f) I_{rms}^2 = \frac{\rho l_z}{\alpha_{sk} l_x} I_{rms}^2 \tag{10}$$

where $R(f)$ is the frequency dependent effective surface resistance (Ω) [11].

The induced current I_{rms} in Eq. (8) is not assumed constant. It results directly from the integration of the frequency dependent current density J_z whose spatial decay depends on the frequency dependent skin depth α_{sk}.

The spatial distribution of the induced current density, and therefore the local power density, is governed by the field geometry, material properties, and the excitation frequency. While the source impedance determines the total current delivered to the source of variable electromagnetic field (Fig. 1), it does not determine how the induced current distributes within the electrically conductive object once the electromagnetic field is established. The depth-wise decay of J_z is dictated solely by the skin depth physics described by Maxwell's equations. This distinction emphasizes that Joule power losses arise from the local field-material interaction, and that the derived expression for P_{loss} properly captures the frequency dependent behavior dictated by electromagnetic induction.

The heat losses from Eq. (10) can be directly related to the temperature rise of the electrically conductive objects. The transient temperature increase of an object is governed by the general heating relation [9]:

$$P_{loss} = m_t C_P \frac{\Delta T}{\Delta t} \tag{11}$$

where m_t is the mass of the object (kg), C_p the specific heat capacity (J/(kg $\cdot$ °K)), ΔT the temperature increment (°K), and Δt the heating duration (s).

Equations (10) and (11) describe the same form of energy conversion, from electrical to thermal. By comparing both, it follows that the temperature rise ΔT of an electrically conductive object is directly proportional to the square of the induced current I_{rms} and to the square root of the operating frequency f:

$$\Delta T \propto \Delta t I_{rms}^2 \sqrt{f} \tag{12}$$

Equation (12) constitutes one of the principal analytical results of this study, establishing a direct energy-frequency coupling for Joule heating produced by variable electromagnetic fields.

The relation can also be expressed in terms of the magnetic energy E stored in the field:

$$E = \frac{LI_{rms}^2}{2} \tag{13}$$

where L is the equivalent inductance of the electromagnetic system (H).

Substituting I_{rms}^2 from Eq. (13) into Eq. (12) gives the general expression

$$\Delta T = \kappa \Delta t E \sqrt{f} \tag{14}$$

where κ is a proportionality constant ($^\circ$K/(J $\cdot$ s$^{1/2}$)) that incorporates material properties, geometry, and the thermal response of the system. It can be expressed as

$$\kappa = \frac{2}{m_t C_p} \frac{\rho l_z}{l_x} \frac{1}{L} \sqrt{\frac{\pi \mu}{\rho}} \tag{15}$$

Equation (14) extends the previous formulation (12) by linking the temperature rise directly to the energy content of the electromagnetic field, thereby serving as a second key contribution of the present work.

Equation (14) quantifies the total electrical energy converted into heat through Joule losses and preserves additive linearity due to the superposition principle and energy conservation in electromagnetic systems [12].

Hence, when multiple frequency components or sources contribute to heating, the total temperature rise can be estimated by summing their respective contributions:

$$\Delta T_{total} = \kappa \Delta t \left(E_1 \sqrt{f}_1 + E_2 \sqrt{f}_2 + \ldots + E_i \sqrt{f}_i \right) \tag{16}$$

Equation (16) represents the third main contribution of this study, generalizing the energy-frequency relation to multiple electromagnetic sources and establishing a framework for cumulative heat generation under complex field spectra.

Furthermore, using proportional reasoning under constant conditions, the relative temperature rise between two different states can be estimated as

$$\frac{\Delta T_2}{\Delta T_1} = \frac{E_2 \sqrt{f}_2}{E_1 \sqrt{f}_1} \tag{17}$$

In other words, if the temperature rise ΔT_1 is known for a given combination of field energy E_1 and frequency f_1, Eq. (17) can be used to predict the temperature rise ΔT_2 corresponding to a new set of parameters E_2, f_2. Determining the values of E_1 and f_1 requires experimental measurements [10]. Alternatively, numerical methods such as the finite element method can be employed to obtain these values [13–15].

The energy-frequency dependence in Eq. (17) provides fundamental framework for describing the thermal energy generated in electrically conductive material without requiring intermediate material parameters [16], marking the fourth principal outcome of this study.

In the next section, Eqs. (16) and (17) are applied to estimate the temperature rise of an electrically conductive object placed within a source of variable electromagnetic field, forming the foundation for analysing how such temperature estimates differ between stationary and moving observers.

3. THERMAL DISCREPANCY BETWEEN MOVING AND STATIONARY OBSERVERS

This section examines how the temperature rise predicted by the energy-frequency dependence (17) differs when the electromagnetic system is in motion relative to the observer. The analysis considers two reference frames:

1. A stationary observer at position X, and
2. A moving observer traveling together with the electromagnetic source.

The aim is to demonstrate that apparent discrepancies in measured temperature arise naturally from the combined effects of the Doppler shift, time dilation, and field contraction, and to introduce the relativistic compensation factor β that reconciles both viewpoints.

3.1. Stationary Observer: Reference State (No Motion)

Suppose that the stationary observer at X performs an experiment with the electromagnetic system shown in Fig. 3. The system delivers a field energy E_1 at frequency f_1.

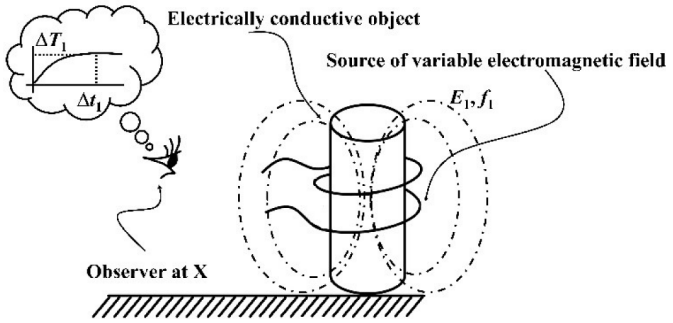

FIGURE 3. Schematic of the measurement setup: a stationary observer at X records the temperature change of an electrically conductive object using a source of variable electromagnetic field with energy E_1 at frequency f_1.

After a time interval Δt_1, the observer at X measures that the conductive object reaches a temperature

$$T_1 = T_0 + \Delta T_1 \tag{18}$$

where T_0 is the initial temperature of the electrically conductive object, and ΔT_1 is the rise predicted by Eq. (14).

3.2. Stationary Observer: Source in Motion

Now consider a second test in which the electromagnetic system moves toward observer at X (Fig. 4). As motion begins, the observed field energy and frequency increase from E_1, f_1 to E_2, f_2 due to the Doppler effect.

After the same nominal duration Δt_1, observer at X would expect the temperature rise to follow Eq. (17), giving a larger

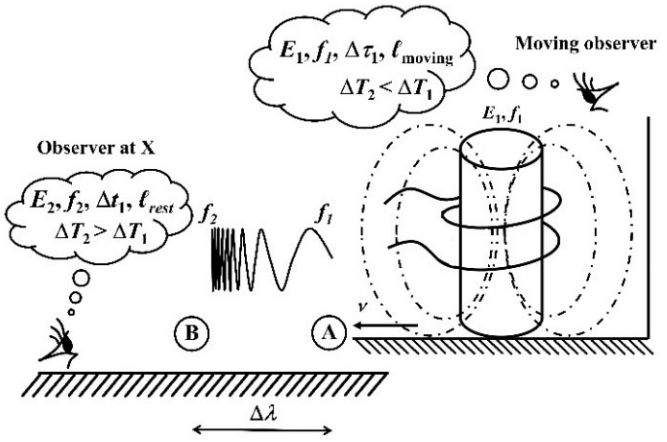

FIGURE 4. From the perspective of observer at X, the measured energy E and frequency f increase due to the Doppler effect.

value than before:

$$\Delta T_2 > \Delta T_1 \tag{19}$$

This prediction, however, is based purely on the Doppler-shifted energy-frequency input and does not yet include relativistic timing effect.

To the stationary observer at X, the electrically conductive object should appear to heat faster due to the higher effective frequency and energy density.

3.3. Moving Observer: Co-Moving Frame of the System

Now consider a second observer moving in tandem with the electromagnetic source (Fig. 4). In this frame, the Doppler effect is absent: the energy and frequency remain E_1, f_1.

The moving observer measures the heating over their own proper time interval $\Delta\tau_1$, which is related to Δt_1 by relativistic time dilation.

From this point of view, the temperature rise is

$$\Delta T_2 = \Delta T_1 \frac{E_1\sqrt{f_1}}{E_1\sqrt{f_1}} \frac{\Delta\tau_1}{\Delta t_1} = \Delta T_1 \frac{\Delta\tau_1}{\Delta t_1} \tag{20}$$

and thus, the final temperature increment satisfies

$$\Delta T_2 < \Delta T_1 \tag{21}$$

because $\Delta\tau_1 < \Delta t_1$ for a moving clock.

Therefore, the moving observer registers a smaller temperature rise than the stationary observer at X would predict.

3.4. Compensation of the Stationary Observer's Estimate

To reconcile the two measurements, the stationary observer at X introduces a dimensionless compensation factor β into Eq. (17):

$$\Delta T_2 = \Delta T_1 \frac{\beta E_2\sqrt{f_2}}{E_1\sqrt{f_1}} \tag{22}$$

The dimensionless factor β must decrease with increasing E_2 and f_2, offsetting the apparent rise caused by Doppler amplification.

The observations of the moving observer and stationary observer at X coincide only when there is no relative motion between them, that is, when the Doppler shift is absent, and the proper time interval equals the coordinate time ($\Delta\tau_1 = \Delta t_1$). When relative motion exists, the factor β compensates for both time dilation and electromagnetic field contraction, thereby ensuring the preservation of energy conservation.

To determine the value of β, the stationary observer at X refers back to the cumulative energy-frequency relation of Eq. (16) from Section 2 and examines the overall energy balance of the system. From this perspective, the observer at X reasons as follows:

If the system had remained stationary, producing an energy E_1 at frequency f_1 over the interval Δt_1, I would have measured a total temperature rise ΔT_1, meaning that 100% of the electromagnetic energy was converted into heat. However, since the source is in motion, I now measure a smaller temperature rise corresponding to $\kappa\Delta t_1\beta E_2\sqrt{f_2}$ after the same elapsed time Δt_1. Therefore, the difference between the ideal stationary contribution and this reduced value must represent the energy discrepancy responsible for the magnitude of the factor β.

Accordingly, from the point of view of the stationary observer at X, the total energy balance of the system can be expressed as

$$\kappa\Delta t_1 E_1\sqrt{f_1} = \left(\kappa\Delta t_1\beta E_2\sqrt{f_2}\right) + \left(\kappa\Delta t_1 E_{disc}\sqrt{f_1}\right) \tag{23}$$

where E_{disc} denotes the energy discrepancy associated with the reduced temperature rise observed during motion.

Isolating E_{disc} from Eq. (23) gives

$$E_{disc} = E_1 - \left(\beta E_2 \frac{\sqrt{f_2}}{\sqrt{f_1}}\right) \tag{24}$$

and dividing Eqs. (20) and (22) yields

$$\beta = \frac{E_1}{E_2}\frac{\sqrt{f_1}}{\sqrt{f_2}}\frac{\Delta\tau_1}{\Delta t_1} \tag{25}$$

The time dilation relation from special relativity [17] provides

$$\Delta\tau_1 = \frac{\Delta t_1}{\gamma}, \tag{26}$$

$$\gamma = \frac{1}{\sqrt{1-\left(\frac{\nu^2}{C^2}\right)}} \tag{27}$$

where ν is the relative velocity, and C is the speed of light (299,792,458 m/s).

The relativistic Doppler effect links the Lorentz factor γ to the observed frequency shift [18]:

$$\gamma = \frac{f_2}{f_1} \tag{28}$$

The derivation of Eq. (28) can be made explicit as follows.

3.5. Explicit Deduction of $\gamma = f_2/f_1$

Because the intensity of an electromagnetic field scales with the cube of the frequency as a Lorentz invariant quantity [19], the following equality holds between the stationary and moving frames:

$$\frac{I_N}{f^3} = \frac{C \cdot E_1}{vol_1 f_1^3} = \frac{C \cdot E_2}{vol_2 f_2^3} \tag{29}$$

where I_N is the intensity of the electromagnetic field (W/m^2), C the speed of light (299,792,458 m/s), and *vol* the volume of space (m^3) occupied by the electromagnetic field distribution.

Rearranging Eq. (29) gives the energy ratio between frames:

$$\frac{E_2}{E_1} = \frac{vol_2}{vol_1}\left(\frac{f_2}{f_1}\right)^3 \tag{29a}$$

Next, the spatial distribution of a moving electromagnetic field contracts along the direction of motion [3, 4]:

$$\ell_{rest} = \frac{\ell_{moving}}{\gamma} \tag{30}$$

where ℓ_{rest} is the contracted dimension measured by the stationary observer at X, and ℓ_{moving} is the corresponding dimension measured by the moving observer (Fig. 4).

Therefore, the total electromagnetic field volume transforms as (see Fig. 5)

$$vol_2 = \frac{vol_1}{\gamma} \tag{31}$$

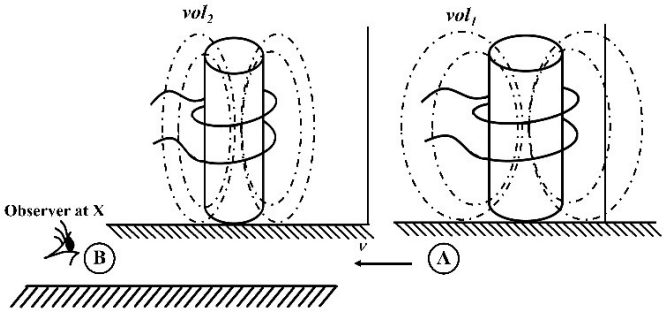

FIGURE 5. Contraction of the electromagnetic field volume along the direction of motion as observed from X.

Substituting Eq. (31) into Eq. (29a) gives

$$\frac{E_2}{E_1} = \frac{1}{\gamma}\left(\frac{f_2}{f_1}\right)^3 \tag{31a}$$

For the total energy and field intensity to remain Lorentz invariant, the factor multiplying E_1 must be reduced to the standard quadratic Doppler scaling of radiant energy $(f_2/f_1)^2$ [11, 20].

This requirement is satisfied only when

$$\gamma = \frac{f_2}{f_1} \qquad \text{(28 revisited)}$$

Thus, Eqs. (29)–(31) jointly ensure that the Lorentz factor equals the frequency ratio term implied by the Doppler effect, preserving the invariance of the electromagnetic energy intensity relationship across frames.

3.6. Substitution into the Energy Discrepancy Relation

Substituting Eqs. (25)–(31) into Eq. (24) yields the expression for the energy discrepancy observed by the stationary observer:

$$E_{disc} = E_1\left(\frac{f_2 - f_1}{f_2}\right) \tag{32}$$

Equation (32) quantifies the energy discrepancy observed by the stationary observer at X, representing the apparent loss of energy that arises due to the combined effects of relativistic field contraction and time dilation.

3.7. Force Associated with Energy-Frequency Redistribution

From the perspective of the stationary observer at X, the moving electromagnetic source in Fig. 4 has expended the energy E_{disc} while traveling from point A to point B. Consequently, the observer concludes that a force must act within the spatial volume vol_2 such that

$$F_c = \frac{E_1}{\Delta\lambda}\left(\frac{f_2 - f_1}{f_2}\right) \tag{33}$$

where F_c is the force (N), and $\Delta\lambda$ is the distance (m) travelled by the electromagnetic system from point A to point B, as measured by the observer at X (Fig. 4).

Additionally, due to the nature of the electromagnetic field, the force in Eq. (33) can be expressed in multiples of Planck's energy as

$$F_c = \frac{Nhf_p}{\Delta\lambda}\left(\frac{f_2 - f_1}{f_2}\right) \tag{34}$$

where h and f_p are the Planck's constant (6.626×10^{-34} J · s) and Planck's frequency (2.952×10^{42} Hz), respectively, and N is the number of units required to match the total electromagnetic energy E_1 such that $E_1 = Nhf_p$.

3.8. Differential form Derived from $\partial E_{disc}/\partial t$

To obtain a continuous representation of Eq. (33), consider the instantaneous frequency of the sweep as $f(t)$. For a small frequency increment Δf, let

$$f_1 = f(t) - \Delta f, \tag{35}$$

$$f_2 = f(t) \tag{36}$$

so that, for an incremental frequency change within the sweep, the term $(f_2 - f_1)/f_2$ in Eq. (33) can be expressed as

$$\left(\frac{f_2 - f_1}{f_2}\right) \approx \frac{1}{f(t)}\frac{df}{dt}dt \tag{37}$$

in the differential limit as $\Delta f \to 0$.

Substituting this relation into Eq. (32) yields $E_{disc} \approx E_1(\Delta f/f(t))$.

Defining the effective force as the rate of change of this energy discrepancy with respect to distance,

$$F_c = \frac{dE_{disc}}{dx} \tag{38}$$

and using $dx = Cdt$ for propagation at the speed of light C, we obtain

$$F_c = \frac{1}{C}\frac{dE_{disc}}{dt} = \frac{E_1}{C}\frac{1}{f\,(t)}\frac{df}{dt} \tag{39}$$

If the sweep extends up to a highest frequency f_H, evaluating the prefactor at $f \simeq f_H$ gives

$$F_c \simeq \frac{E_1}{Cf_H}\frac{df}{dt} \tag{40}$$

Substituting $E_1 = Nhf_p$ into Eq. (40) yields the general differential form

$$F_c = \frac{Nh}{C}\frac{f_p}{f_H}\left(\frac{\partial f}{\partial t}\right) \tag{41}$$

3.9. Clarification on the Physical Interpretation of $\mathbf{F_c}$

To establish a direct link between the electromagnetic field formulation and the effective force F_c, we start from Poynting's theorem, which expresses the local conservation of electromagnetic energy as

$$\nabla \cdot \mathbf{S} + \frac{\partial U_{EM}}{\partial t} = -\mathbf{J} \cdot \mathbf{E} \tag{42}$$

where $U_{EM} = (1/2)(\varepsilon_0|\mathbf{E}|^2 + \mu_0|\mathbf{H}|^2)$ is the electromagnetic energy density (J/m^3), and $\mathbf{S} = \mathbf{E} \times \mathbf{H}$ is the Poynting vector representing the electromagnetic energy flux density (W/m^2). Here, $|\mathbf{E}|$ denotes the magnitude of the electric field strength (V/m), $|\mathbf{H}|$ the magnitude of the magnetic field intensity (A/m), and $\mathbf{J}$ the conduction current density vector (A/m^2) describing the local flow of charge interacting with the field.

When the excitation frequency varies in time, $f = f(t)$, both $\mathbf{E}$ and $\mathbf{H}$ acquire explicit frequency dependence, producing an additional temporal contribution to the energy density term,

$$\frac{\partial U_{EM}}{\partial t} = \frac{\partial U_{EM}}{\partial f}\frac{\partial f}{\partial t} \tag{43}$$

Integrating this expression over the interaction volume V (m^3) gives the total electromagnetic energy variation rate,

$$\frac{dE}{dt} = \int_V \frac{\partial U_{EM}}{\partial f}\frac{\partial f}{\partial t}dV \tag{44}$$

Because the electromagnetic field carries linear momentum $p = E/c$ (kg · m/s), the corresponding inertial reaction exerted on the surrounding medium is obtained by dividing the energy rate term by the propagation speed C,

$$F_c = \frac{1}{C}\frac{dE}{dt} \tag{45}$$

This formulation verifies that F_c has the correct dimensional form of a force (N=kg · m/s^2) and shows that it follows directly from the field energy-momentum relation implied by Poynting's theorem. Importantly, this establishes Eq. (41) as a field based inertial force, not a proportional assumption.

To clarify this role in the derivation, the quantity

$$E_{disc} = \int_V \Delta U_{EM} dV \tag{46}$$

is explicitly defined as the total electromagnetic energy discrepancy (J) between the stationary and moving observers, arising from relativistic time dilation and field contraction.

Its time derivative dE_{disc}/dt, therefore, represents the rate of change of the electromagnetic energy imbalance, which by energy-momentum equivalence corresponds directly to a momentum flux rate. The effective inertial force

$$F_c = \frac{1}{C}\frac{dE_{disc}}{dt} \tag{47}$$

thus expresses the field mediated momentum transfer associated with a frequency sweep. Therefore, F_c does not represent a mechanical contact force but an *effective inertial force* perceived by the stationary observer at X. It quantifies the momentum transfer that results from the relativistic redistribution of electromagnetic energy during a frequency sweep; that is, during temporal modulation of the field frequency.

Accordingly, Eq. (28) must be understood as including the contribution of field momentum, which is embedded in the Poynting vector term of the conservation law. Energy transformations between observers therefore involve both electromagnetic energy density and momentum flux.

This interpretation confirms the dimensional consistency of E_{disc} (J), its origin in electromagnetic energy density U_{EM} (J/m^3), and the physical basis of F_c as a relativistic inertial response perceived by the stationary observer during a frequency sweep.

Equation (41) predicts that a moving source of variable electromagnetic field generates a force in the reference frame of a stationary observer, such as the observer at X in Fig. 4. This force arises from the combined effects of length contraction and time dilation, which act to preserve the principle of energy conservation. Furthermore, owing to the traveling nature of electromagnetic waves, Eq. (41) implies that a stationary observer cannot distinguish between a frequency sweep produced by a moving source and a frequency sweep produced by a stationary source through internal modulation (Fig. 6).

A similar phenomenon was described by Searle [4], who showed that the spatial distribution of the electric field produced by a charged ellipsoid can be explained either with or without introducing relative motion between the charged body

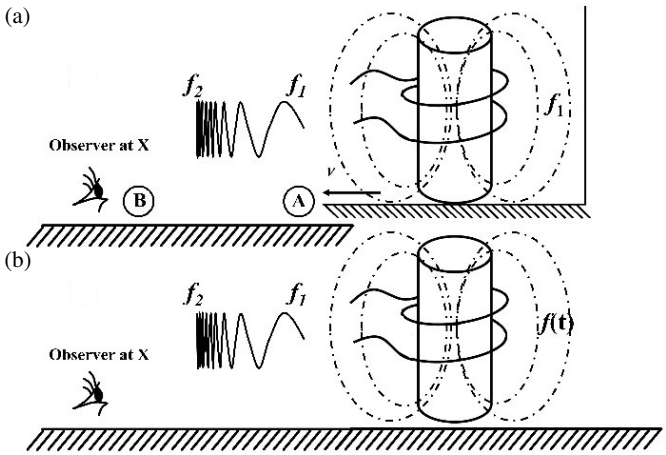

FIGURE 6. From the perspective of a stationary observer, a frequency sweep in an electromagnetic field may be indistinguishable whether produced by (a) a moving source of variable electromagnetic field or (b) a traveling electromagnetic wave of variable frequency (temporal modulation of field frequency).

and a stationary observer. From the stationary observer's perspective, there is not fundamental difference between a sweep caused by relative motion and one induced internally.

Consequently, the mechanical effect described by Eq. (41) must arise independently of the sweep's origin, reinforcing the concept of a frame-invariant inertial force resulting from energy-frequency redistribution.

This interpretation aligns with earlier analysis of reactive near-field energy and internal electromagnetic energy flow in radiating systems. In particular, studies on dipole antennas and localized emitters have shown that oscillatory storage and release of electromagnetic energy in the near-field give rise to momentum exchange even in the absence of radiation pressure [21, 22]. The present formulation extends those interpretations to dynamic frequency sweep conditions, where temporal modulation of field frequency produces a similar exchange mechanism governed by relativistic contraction and time dilation.

Moreover, the effect described in Eq. (41) may be enhanced in regions where the field geometry contains edges or pin-like singularities, as these configurations concentrate reactive energy and amplify local field gradients [23, 24]. Such geometrical amplification would increase the apparent inertial response F_c experienced by nearby materials, providing a potential experimental pathway for detecting frequency sweep induced forces in practical systems.

The general expression in Eq. (41) thus indicates that the speed of a frequency sweep in an electromagnetic wave can produce a relativistic effect, perceived as a force by stationary electrically conductive objects.

The following section examines the physical implications of the interaction between the force F_c and the mass of stationary, non-electrically conductive objects.

4. F_c IN RELATION TO RELATIVISTIC INERTIA AND FIELD-INDUCED MASS INTERACTIONS

The force F_c parallels the relativistic forces observed when a mass moves relative to a stationary reference frame.

According to the theory of relativity, the mass of a moving object increases relative to a stationary observer, as given by:

$$m = m_0\gamma \tag{48}$$

where m_0 is the rest mass (kg) of the moving object, and m is the relativistic mass (kg) as measured by a stationary observer.

Suppose that an object of rest mass m_0 travels from point A to point B at velocity ν relative to a stationary observer (Fig. 7). Before the object is set in motion, the stationary observer verifies that its rest energy is

$$E_{m0} = m_0C^2 \tag{49}$$

where E_{m0} is the rest energy (J) [25].

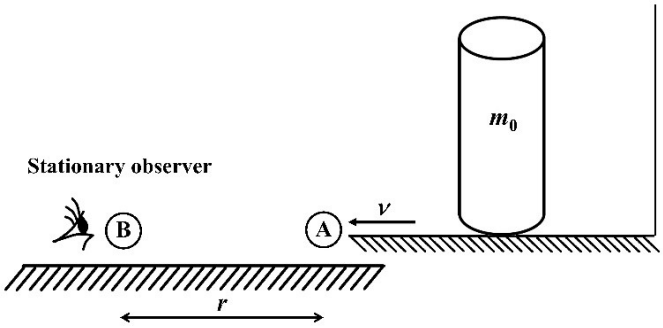

FIGURE 7. Object of rest mass m_0 located at point A prior to motion toward point B relative to a stationary observer.

Once the object moves, its total energy increases according to the relativistic mass relation in Eq. (48):

$$E_{mtot} = \gamma m_0C^2 \tag{50}$$

where E_{mtot} is the total energy of the moving object (J).

Relative motion also produces a contraction of the object's spatial dimension along the direction of travel (Lorentz–Fitzgerald contraction). From the stationary observer's perspective, this contraction can be associated with stored energy E_f, produced by a relativistic force F_f acting on the object's volume and surrounding space (Fig. 8). As the object accelerates from A to B, the stored energy E_f increases.

By energy conservation, the sum of the stored energy E_f and the rest energy E_{m0} in Eq. (49) must equal the total energy E_{mtot} in Eq. (50):

$$E_{mtot} = E_f + E_{m0} \tag{51}$$

Expressing Eq. (51) in terms of $m0$ and isolating the stored energy E_f gives

$$E_f = \gamma m_0C^2 - m_0C^2 \tag{52}$$

Now it is possible to define an effective force F_f as the rate of change of the stored energy E_f with respect to distance r (m) from A to B:

$$F_f = \frac{dE_f}{dr} = \frac{d}{dr}\left(\gamma m_0C^2 - m_0C^2\right) \tag{53}$$

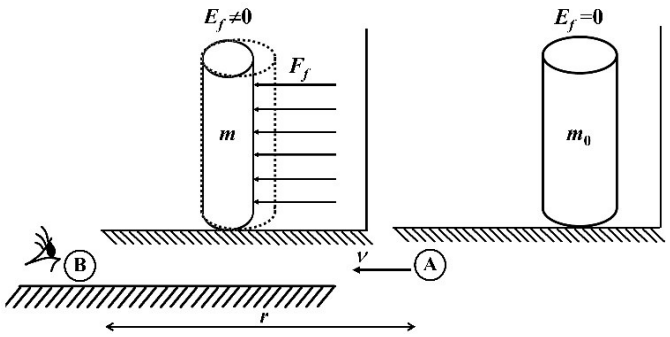

FIGURE 8. Stationary observer describes Lorentz-Fitzgerald contraction of a moving object as a stored energy E_f arising from a relativistic force F_f acting along the travel distance r.

Since the rest energy E_{m0} is constant, Eq. (53) reduces to

$$F_f = \frac{dE_f}{dr} = m_0 C^2 \frac{d\gamma}{dr} \tag{54}$$

Using $\gamma = (1 - v^2/C^2)^{-1/2}$ and applying the chain rule gives $d\gamma/dt = \gamma^3(va)/C^2$ (where a is acceleration (m/s^2)). Therefore, considering that $dr/dt = v$ and substituting these expressions into Eq. (54), we obtain

$$F_f = \gamma^3 m_0 a \tag{55}$$

Equation (55) is the relativistic expression for inertial force acting on a mass accelerated in the direction of motion [26, 27]. In the low velocity limit $\nu << C$, it reduces to the classical expression $F_f \approx m_0 a$, while at relativistic speeds it increases sharply with γ^3, reflecting the well-known growth of inertial resistance with velocity [26, 27].

Crucially, F_f exhibits the same energy-space coupling (a force as an energy gradient) that underlies the definition of F_c. In both cases, Lorentz-Fitzgerald contraction and time dilation reshape energy densities so that energy-momentum conservation holds across frames

This motivates the introduction of a dimensionless proportionality constant α that parametrizes how the field sweep forces acting on conductive targets (F_c) produce a corresponding inertial response in neutral, non-conductive matter (F_{cf}):

$$F_{cf} = \alpha F_c \tag{56}$$

where α is a dimensionless coupling constant, and F_{cf} denotes the inertial force exerted by the frequency sweep of an electromagnetic wave on non-electrically conductive matter.

This proportional relationship is not arbitrary but reflects that F_f and F_c are dual manifestations of the same relativistic mechanism.

Both forces F_f and F_c originate from the same Lorentzian modification of energy density (one acting on mass-energy, the other on field-energy) to preserve energy conservation in the stationary frame.

This equivalence forms the foundation for Section 5, where physically justified bounds for α are established and the broader physical implications of this inertial coupling are explored.

5. PHYSICALLY GROUNDED BOUNDS FOR α AND IMPLICATIONS

The proportionality constant α, introduced in Eq. (56), quantifies how the field sweep force F_c acting on electrically conductive materials extends to neutral, non-conductive matter as $F_{cf} = \alpha F_c$.

Because both forces originate from the same Lorentzian transformation of energy density, α must be determined from measurable physical quantities rather than arbitrary scaling.

5.1. Derivation of the Coupling Scale

For neutral matter, the microscopic coupling between field and mass is governed by the relative strength of gravitational and electromagnetic interaction for the elementary charge carriers.

The natural dimensionless ratio between these two forces is

$$\chi(m, q) = \frac{F_G}{F_E} = \frac{G m_p^2}{\kappa_e q^2} \tag{57}$$

where F_E and F_G are the magnitudes of the electric and gravitational forces (N), $G = 6.674 \times 10^{-11}$ Nm^2/kg^2 is the gravitational constant, $\kappa_e = 8.988 \times 10^9$ Nm^2/C^2 is Coulomb's constant, m_p is the particle mass (kg), and q its charge (C).

For the electron ($m_p = 9.11 \times 10^{-31}$ kg, $q = 1.602 \times 10^{-19}$ C),

$$\chi_e \approx 2.4 \times 10^{-43} \tag{58}$$

For the proton ($m_p = 1.67 \times 10^{-27}$ kg, $q = 1.602 \times 10^{-19}$ C),

$$\chi_p \approx 8 \times 10^{-37} \tag{59}$$

This microscopic strength ratio provides a universal physical lower scale for how weakly neutral matter can couple to electromagnetic fields through polarization of its bound charges. To represent macroscopic response, a polarization overlap factor $\Phi \in (0, 1]$ is introduced to account for geometry, screening, and detuning from resonance.

The neutral matter coupling coefficient therefore follows as

$$\alpha = \chi \Phi \tag{60}$$

5.2. Physically Justified Range of α

For off-resonant, non-conductive solids, the polarization factor is small ($\Phi \sim 10^{-2}$–10^{-3}). Substituting Eq. (58) gives

$$\alpha_{\min} \approx \chi_e \Phi \sim \left(2.4 \times 10^{-43}\right) \times \left(10^{-2} - 10^{-3}\right)$$

$$\Rightarrow \alpha_{\min} \approx 10^{-45} \tag{61}$$

For moderate dielectric response or partial field overlap ($\Phi \sim 10^{-1}$) and an average microscopic ratio $\chi \sim 10^{-40}$ yields

$$\alpha_{\max} \approx 10^{-39} \tag{62}$$

Thus, for ordinary materials and non-resonant electromagnetic sweeps, α lies robustly within the physically justified range

$$10^{-45} \lesssim \alpha \lesssim 10^{-39} \tag{63}$$

5.3. Interpretation

Equation (60) shows that α is not a fitting constant but a measurable ratio linking gravitational-electromagnetic strength of microscopic carriers (χ) to the macroscopic polarization response (Φ). It represents how efficiently the frequency sweep field's energy density gradient transfers to inertial mass in neutral medium.

The range in Eq. (63) ensures that $F_{cf} = \alpha F_c$ remains many orders of magnitude smaller than F_c for ordinary matter, consistent with the absence of observable motion in typical laboratory fields, yet preserves a finite, physically meaningful coupling compatible with relativistic energy conservation.

5.4. Thermodynamic Form of α and Final Expression for F_{cf}

The coupling constant can also be expressed in terms of thermodynamic energy scales to emphasize its universality.

If the maximum field mass coupling is limited by the Planck temperature $T_p = 1.416784 \times 10^{32}$°K and Boltzmann's constant $\kappa_B = 1.380649 \times 10^{-23}$ J/°K, while the total field energy available for conversion is E_v (J), then

$$\alpha = \frac{\kappa_B T_p}{E_v} \tag{64}$$

For characteristic cosmological or laboratory energy scales $E_v \sim 10^{48} - 10^{54}$ J, this ratio yields $\alpha \sim 10^{-45}$–10^{-39}, consistent with the range in Eq. (63).

Substituting Eq. (64) into Eq. (56) gives

$$F_{cf} = \frac{Nh}{C} \frac{f_p}{f_H} \left(\frac{\partial f}{\partial t} \right) \frac{\kappa_B T_p}{E_v} \tag{65}$$

Or equivalently, in terms of the total electromagnetic field energy E_e

$$F_{cf} = \frac{E_e}{C f_H} \left(\frac{\partial f}{\partial t} \right) \frac{\kappa_B T_p}{E_v} \tag{66}$$

Equations (65)–(66) show that the frequency sweep of an electromagnetic wave can generate an inertial type force acting on any mass, independent of electrical conductivity. This force arises fundamentally from relativistic length contraction and time dilation, ensuring energy conservation in the stationary reference frame

6. POTENTIAL DETECTION METHODS AND APPLICATIONS

Detecting F_{cf} would require either strong sweep fields, very light test masses, or resonance conditions that enhance Φ.

The predicted range of α implies that measurable effects may become significant only in high intensity or near resonant regimes, guiding the design of future experiments.

The inertial force F_{cf} predicted in this work could be investigated using ultra-sensitive interferometers, microbalances, or particle tracking systems in high-vacuum environments.

A representative test would suspend a neutral dielectric particle in vacuum and exposed it to a tunable electromagnetic field undergoing a frequency sweep. Any displacement not attributable to radiation pressure or electrostatic forces would constitute direct evidence of F_{cf}.

Beyond detection, the nature of F_{cf} suggests novel applications. In space propulsion, internal frequency sweep fields could provide thrust for compact, long duration propulsion systems. In nanotechnology or biomedicine, the same effect could enable manipulation of neutral particles or biomolecules with high precision and minimal heating.

More broadly, the confirmation of F_{cf} would open new avenues for studying relativistic field-mass coupling and could contribute to emerging frameworks connecting inertia, information, and electromagnetic structure.

6.1. Experimental Constraint Example

For a total field energy $E_e = 10^{-3}$ J and a sweep rate of 10^{11} Hz/s, a force sensor with threshold $F_{\min}$ constrains

$$\alpha \leq \frac{F_{\min}}{E_e \cdot 10^{11}\ \text{Hz/s}} \tag{67}$$

For $F_{\min} = 10^{-14}$ N (a sensitivity achievable by modern optical microbalances [28]), the experiment would set $\alpha \leq 10^{-22}$. This limit remains many orders of magnitude larger than the theoretical range $10^{-45} \lesssim \alpha \lesssim 10^{-39}$; hence, a null result would not yet challenge the theory whereas a measurable signal near that threshold would demand a re-evaluation of the coupling scale α.

7. CONCLUSIONS

We conclude that the frequency sweep of an electromagnetic wave produces an inertial force F_{cf} that interacts with the mass of objects, independent of their electrical properties. This force arises from the combined effects of Lorentz–Fitzgerald contraction and time dilation, ensuring the preservation of energy conservation between electrical and thermal measurements obtained by both stationary and moving observers. The equivalence between F_{cf} and relativistic inertial forces suggests a fundamental link between electromagnetic frequency modulation and mass–energy interactions, with potential for experimental verification and technological application.

Furthermore, the present formulation interprets F_c and F_{cf} as differential manifestations of energy-momentum conservation within Lorentz transformed geometries. Future work will extend this framework to the full covariant formulation of the electromagnetic stress-energy tensor, allowing the force relations developed here to be expressed directly in tensorial form. This will establish a deeper connection between the suggested inertial effects produced by frequency sweeps and the general relativistic description of energy-momentum flow in spacetime.

REFERENCES

[1] Peregoudov, D. V., "Relativistic length contraction and time dilation as dynamical phenomena," *European Journal of Physics*, Vol. 41, No. 1, 015602, Dec. 2019.

[2] Redžić, D. V., "Image of a moving sphere and the FitzGerald-Lorentz contraction," *European Journal of Physics*, Vol. 25, No. 1, 123, 2004.
[3] Heaviside, O., "XXXIX. On the electromagnetic effects due to the motion of electrification through a dielectric," *The London, Edinburgh, and Dublin Philosophical Magazine and Journal of Science*, Vol. 27, No. 167, 324–339, 1889.
[4] Searle, G. F. C., "On the steady motion of an electrified ellipsoid," *Proceedings of the Physical Society of London*, Vol. 15, No. 1, 264, 1896.
[5] Le Bellac, M. and J. M. Lévy-Leblond, "Galilean electromagnetism," *Il Nuovo Cimento B (1971-1996)*, Vol. 14, No. 2, 217–234, Apr. 1973.
[6] De Montigny, M. and G. Rousseaux, "On the electrodynamics of moving bodies at low velocities," *European Journal of Physics*, Vol. 27, No. 4, 755, 2006.
[7] Harsha, N. R. S., A. Prakash, and D. P. Kothari, *The Foundations of Electric Circuit Theory*, IOP Publishing, 2016.
[8] Koivurova, M., C. W. Robson, and M. Ornigotti, "Time-varying media, relativity, and the arrow of time," *Optica*, Vol. 10, No. 10, 1398–1406, 2023.
[9] Incropera, F. P. and D. P. DeWitt, *Fundamentos de Transferencia de Calor*, 4th ed., Prentice Hall, 1999.
[10] John, D. and P. Simpson, *Induction Heating Handbook*, McGraw-Hill, 1979.
[11] Jackson, J. D., *Classical Electrodynamics*, 3rd ed., Wiley, 2021.
[12] Ulaby, F. T. and U. Ravaioli, *Fundamentals of Applied Electromagnetics*, Pearson Education UK, 2015.
[13] Ovando-Martinez, R. B. B., C. Hernandez, and M. A. Arjona, "An adaptive time-stepping algorithm in weakly coupled electromagnetics-thermal-circuit modeling," *Applied Computational Electromagnetics Society Journal (ACES)*, Vol. 28, No. 9, 871–878, Sep. 2021.
[14] Ovando-Martinez, R. B. B., M. A. A. Lopez, and C. H. Flores, "A finite-element variable time-stepping algorithm for solving the electromagnetic diffusion equation," *IEEE Transactions on Magnetics*, Vol. 48, No. 2, 647–650, Feb. 2012.
[15] Hernandez, C., R. B. B. Ovando-Martinez, and M. A. Arjona, "Application of tensor analysis to the finite element method," *Applied Mathematics and Computation*, Vol. 219, No. 9, 4625–4636, Jan. 2013.
[16] Ovando, R. B. B., "Apparatus and method for leakage electromagnetic field sensing in electrical inductive equipment," US Patent 11,047,895, 2021.
[17] Misner, C. W., K. S. Thorne, and J. A. Archibald, *Gravitation*, W. H. Freeman and Company, 1973.
[18] Thim, H. W., "Absence of the relativistic transverse Doppler shift at microwave frequencies," *IEEE Transactions on Instrumentation and Measurement*, Vol. 52, No. 5, 1660–1664, Oct. 2003.
[19] Johnson, M. H. and E. Teller, "Intensity changes in the Doppler effect," *Proceedings of the National Academy of Sciences*, Vol. 79, No. 4, 1340, Feb. 1982.
[20] Rindler, W., *Introduction to Special Relativity*, 2nd ed., Oxford University Press, 1991.
[21] Valagiannopoulos, C. A. and A. Alú, "The role of reactive energy in the radiation by a dipole antenna," *IEEE Transactions on Antennas and Propagation*, Vol. 63, No. 8, 3736–3741, Aug. 2015.
[22] Lee, H.-I., "Near-field behaviors of internal energy flows of free-space electromagnetic waves induced by electric point dipoles," *Optics*, Vol. 3, No. 3, 313–337, Sep. 2022.
[23] Braver, I. M., P. S. Fridberg, K. L. Garb, and I. M. Yakover, "Electromagnetic field near the common edge of a perfectly conducting wedge and a resistive half-plane," *ArXiv Preprint ArXiv:2408.13916*, 2024.
[24] Valagiannopoulos, C. A., "On smoothening the singular field developed in the vicinity of metallic edges," *International Journal of Applied Electromagnetics and Mechanics*, Vol. 31, No. 2, 67–77, Oct. 2009.
[25] Einstein, A., "Does the inertia of a body depend upon its energy-content," *Annalen Der Physik*, Vol. 18, No. 13, 639–641, 1905.
[26] Tolman, R. C., *The Theory of the Relativity of Motion*, University of California Press, 1917.
[27] Rindler, W., *Relativity: Special, General, and Cosmological*, Oxford University Press, 2006.
[28] Stoev, I. D., B. Seelbinder, E. Erben, N. Maghelli, and M. Kreysing, "Highly sensitive force measurements in an optically generated, harmonic hydrodynamic trap," *eLight*, Vol. 1, No. 1, 7, Dec. 2021.